Oil & Gas Science and Technology – Rev. IFP Energies nouvelles **76**, 58 (2021)

https://doi.org/10.2516/ogst/2021040

Available online at:
ogst.ifpenergiesnouvelles.fr

REGULAR ARTICLE

OPEN ACCESS

Static and flow behaviors of supercritical CO_2 foam stabilized with betaine surfactant for mobility control application

Weitao Li[1,*], Kai Wang[2], and Wenkuan Zheng[1]

[1] Research Institute Exploration and Development, Shengli Oilfield Company, SINOPEC, Dongying City, Shandong Province, 257015, PR China
[2] Research Institute of CNOOC, Beijing City, 100027, PR China

Received: 10 January 2021 / Accepted: 6 July 2021

Abstract. Aiming at improving the stability of supercritical CO_2 (SC-CO_2) foam in high temperature and salinity reservoirs, a kind of betaine surfactant, Hexadecyl Hydroxypropyl Sulfo Betaine (HHSB), was screened to stabilize SC-CO_2 foam. The properties of SC-CO_2 foam were improved at elevated temperature and pressure. The effects of surfactant concentration, temperature, pressure and salinity on film drainage rate were measured to explore the stability of SC-CO_2 foam. The results showed that an increase of surfactant concentration, pressure and salinity can decrease film drainage rate and enhance the foam stability, which was attributed to the increase of surfactant adsorption at the gas–liquid interface. The performance of SC-CO_2 foam formed by HHSB was improved and the tolerant temperature was up to 100 °C. 1-D core flooding experiments indicated that compared with Coinjection of Surfactant and Gas (CSG) method the SC-CO_2 foam generated through Surfactant-Alternative-Gas (SAG) method had lower foam strength but better in-depth migration capacity. The high temperature and pressure 3-D sand showed that in Water-Alternative-Gas (WAG) case CO_2 broke early through the high permeability layers. In SAG case, SC-CO_2 foam can improve the macroscopic sweep efficiency by reducing the CO_2 mobility.

1 Introduction

CO_2 flooding has been becoming a popular EOR (enhanced oil recovery) method in the low-permeability reservoirs (Ghasemi *et al.*, 2018; Patil *et al.*, 2018). At reservoir conditions, CO_2 can be easily dissolved in the crude oil to expand the net volume of oil and reduce the oil viscosity (Emera and Sarma, 2005). However, early gas breakthrough led to low oil recovery efficiency due to reservoir heterogeneity, the severe channeling and gravity override caused by unfavorable mobility and density contrast (Al Ayesh *et al.*, 2017; Ren *et al.*, 2018). In order to lower the gas mobility and improve the vertical and horizontal sweep efficiency, CO_2 foams stabilized by surfactants were applied in some EOR process (Friedmann *et al.*, 1991; Rossen *et al.*, 2010). Foam could decrease the mobility of CO_2 by reducing the relative permeability and increasing apparent viscosity, thereby diverting CO_2 into the parts of the reservoirs that were previously unwept (Li *et al.*, 2006). When CO_2 and aqueous solution were mixed in the porous media, generated Supercritical CO_2 (SC-CO_2) foam could cause high trapped-gas saturation in porous media, which would lead to the reduction of gas relative permeability. On the other hand, the apparent gas viscosity was increased because the foam flow was blocked by drag force along the pore walls (Hirasaki and Lawson, 1985). The foam rheology was controlled by the bubble texture (lamellae density), which was determined by the generation, trapping and coalescence of the flowing foam (Du *et al.*, 2018).

In order to acquiring long-lasting foam, surfactants must be added to aqueous solutions to act as foam stabilizer. The adsorption of surfactant at gas–liquid interface would protect the bubble film from rapid thinning and breakage. Considering lower adsorption on rocks, temperature resistance and salt tolerance, surfactant was screened to stabilize the foam films (Heller and Kuntamukkula, 1987). For instance, anionic surfactants, such as Sodium Dodecyl Sulfate (SDS), Alpha Olefin Sulfonate (AOS) and Sodium Dodecylbenzene Sulfonate (SDBS) would interact with divalent cations to form precipitation under high salinity conditions (Ge and Wang, 2015). In recent years, betaine surfactant, a kind of zwitterionic surfactant, has attracted great attention because of its good salinity tolerance and foaming capacity (Da *et al.*, 2018). Betaine surfactants were usually mixed with anionic surfactants as foam boosters to enhance foam stability at harsh conditions

* Corresponding author: liweitao128@163.com

(Basheva *et al.*, 2000; Li *et al.*, 2012). Addition of betaine surfactants could change the interfacial properties at the C-W interface and CO_2 foams become very stable. The adsorption of surfactant at the interface will lead to some surface properties, such as surface viscosity, surface elasticity and surface tension. These surface properties will affect the lamellae stability. For example, increase of surface viscosity will reduce the foam lamellae drainage rate. Higher surface elasticity of will dampen the surface fluctuations and resist the external interference, such as capillary pressure, temperature and oil. Surface tension was determined by the degree of surfactant adsorption. Higher surfactant adsorption and lower interfacial tension will reduce the formation of open holes at the interface, which will increase the coalescence rate of SC-CO_2 foam (Golemanov *et al.*, 2008). Danov *et al.* (2004) have verified that addition of betaine surfactant could considerably increase film elasticity and improve the foam stability with the Wilhelmy plate method.

Although a large number of scholars have studied the CO_2 foam, the previous study was mainly conducted at atmospheric pressure and the dissolved amount of CO_2 in aqueous solution was lower (Wang and Yoon, 2009). Some key problems of supercritical CO_2 foam under high temperature and pressure have not yet been solved. Under high temperature and pressure, the change of chemical properties of CO_2 will inevitably affect the application of CO_2 foam in oil reservoirs (Holt *et al.*, 1996). Besides, at high pressure the surfactant solution was acidic, which will affect the properties of surfactant (Xue *et al.*, 2016). It was reported that the pH value of the water–CO_2 binary system was approximately 3 as the pressure was increased to 8 MPa (Li *et al.*, 2019) Therefore, the study of supercritical CO_2 foam under high temperature and pressure is of great theoretical value and application significance.

In our laboratory, a zwitterionic surfactant, Hexadecyl Hydroxypropyl Sulfo Betaine (HHSB) was screened to stabilize CO_2 foam at high salinity and temperature. It was known that the foam stability was mainly affected by lamellae drainage and gas diffusion between bubbles. However, few researches were conducted to measure the lamellae drainage rate to investigate foam stability systematically at elevated pressure. First, high pressure will affect the dissolved amount of CO_2, thereby influencing the pH of aqueous solution. Secondly, high pressure will affect the properties of surfactant molecules, thereby influencing the adsorption of surfactant on the gas–liquid interface. Thirdly, high pressure will decrease the density difference between water and CO_2, thereby influencing the foam stability at high temperature. Based on the above problems, the drainage rate and interfacial tension of SC-CO_2 foams were also explored as a function of different parameters, including temperature, pressure, salinity and surfactant concentration. The flow behaviors of SC-CO_2 foam were studied by using 1-D core flooding for both Surfactant-Alternative-Gas (SAG) and Coinjection of Surfactant and Gas (CSG). A heterogeneous 3-D sand tank was prepared to explore the mobility control ability of SC-CO_2 foam under high temperature and pressure conditions. Because oil can be very detrimental to foam, all the work has been carried out in the absence of oil.

2 Experimental

2.1 Materials

The betaine surfactant, HHSB $C_{16}H_{33}N(CH_3)_2CH_2CH(OH)CH_2SO_3$, was donated by the *Shanghai Nuosong Chemical Co., Ltd.*, China. The surfactant concentration was set at 0.3%. Sodium chloride and calcium chloride were purchased from Beijing Chemical Works, China. Formation brine was prepared using deionized (DI) water with the addition of NaCl and $CaCl_2$ with a 9:1 ratio and the salinity ranged from 2×10^4 mg/L to 25×10^4 mg/L.

2.2 SC-CO_2 foaming stability and microstructure assessment

The foam stability and microstructure of SC-CO_2 foam were evaluated by using a High-Temperature High-Pressure (HTHP) foaming apparatus (Fig. 1) at 70 °C and 8 MPa (Farid Ibrahim and Nasr-El-Din, 2018). The preparation procedure of the SC-CO_2 foam was mainly described as the following: First, a 100 mL surfactant solution was pumped into the HTHP view chamber from the bottom. Secondly, the gas storage tank inside the oven was pressurized to 15 MPa and heated to 70 °C by using the gas boost pump. Thirdly, CO_2 in the gas storage tank was allowed into the HTHP view chamber from the bottom until it reached a specific pressure. When the temperature in the view chamber was stable at 70 °C, the surfactant solutions were agitated at a speed of 2000 rpm for 5 min. Finally, we will record the maximum foaming volume and drainage volume with time to evaluate the foaming ability and calculate the drainage rate. The foaming and drainage processes were shown in Figure 2. The foam generated by high speed stirring method was poured into the high pressure optical cell with a path length of 100 μm which was mounted on a microscope (Leica S6D). After the optical cell was filled with foam (Fig. 3a), the valves on both ends of optical cell were closed. The images of the SC-CO_2 foams were recorded using a microscope camera that was connected to a computer to observe the effluent foam textures (Fig. 3b).

2.3 Foam strength and in-depth migration in the porous media

The foam strength and in-depth migration in the porous media were investigated through multi-point pressure measurement experiment at 70 °C and 8 MPa. Figure 4 showed the schematic of the experiment setup for multi-point pressure test. The core with a diameter of 25 mm was 30 cm long and the core holder was equipped with three pressure taps which was used to determine the pressure drops across the core sample at certain distance. The foam injection was conducted with two methods including: SAG and CSG. The total flow rate, temperature and back pressure were respectively set at 5 mL/min, 70 °C and 8 MPa. The gas–liquid ratio was 1:1 in the injection process. The detailed experimental procedures were displayed in the report of Li *et al.* (2019).

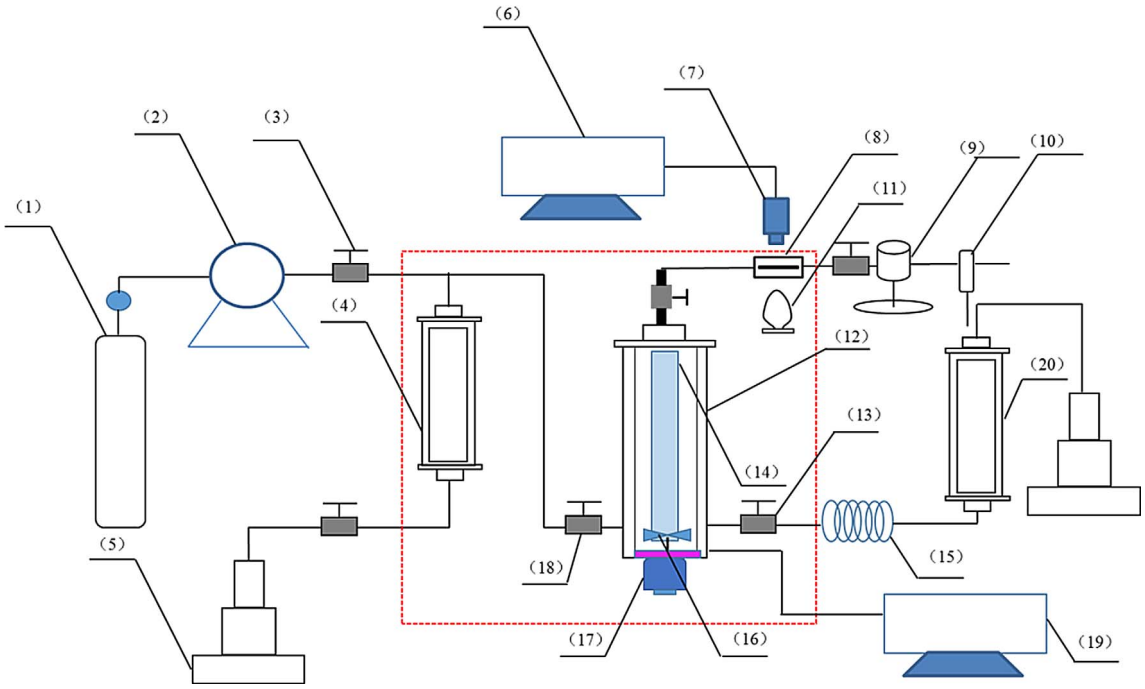

Fig. 1. Schematic of apparatus used for foaming stability and microstructure evaluation. (1) CO_2 gas tank; (2) Gas booster pump; (3) Gas inlet valve; (4) CO_2 intermediate container; (5) ISCO pump; (6) Computer using for imaging; (7) Microscope; (8) High-pressure optical cell; (9) Back pressure regulator; (10) Gas–liquid separator; (11) LED light; (12) High-pressure view chamber; (13) Liquid inlet valve; (14) Sapphire glass; (15) Heat exchanger; (16) Mixing blade; (17) Electric motor; (18) Gas inlet valve; (19) Computer using for control; (20) Liquid intermediate container.

2.4 The bulk viscosity of surfactant solution at high temperature and pressure

The bulk viscosity of surfactant solutions was important for the foam stability. First, increase of bulk viscosity can lead to larger film viscosity, which could reduce the drainage rate of film. Secondly, increase of bulk viscosity can lead to higher interface viscosity, which can lead to improve the stability of gas–liquid interface. The apparent viscosity of the surfactant solutions was measured using a Cambridge HTHP viscometer at 70 °C and 8 MPa. After the sampling chamber was heated to the desired temperature, the surfactant solutions with different salinities were pumped into the cell until it reached the desired pressure. Finally, the measurements started automatically. The measurements ignored the effect of CO_2 on the viscosities of the surfactant solutions.

2.5 Interfacial tension measurements under HTHP conditions

The Interfacial Tension (IFT) values between CO_2 and different surfactant solutions were measured with an HTHP interfacial tensiometer (*ramé-hart Instrument*, France). The values of the IFT were obtained using image analysis software. Determination of the IFT for every measurement was repeated three times, and the average value was calculated. Due to the relatively low mutual solubility of water and CO_2, the pure component density was used for the calculation. The IFT was calculated by the following equation (1):

$$\gamma = \Delta\rho g R_0^2 / \beta, \tag{1}$$

where γ is the surface tension, $\Delta\rho$ is the mass density difference between the surfactant solution and CO_2, R_0 is the radius of curvature at the drop apex, and β is the shape factor.

2.6 The mobility control of supercritical CO_2 foam in homogeneous 3-D sand packing tank

In order to evaluate the ability of HHSB to reduce the mobility of SC-CO_2, a HTHP sand packing tank was designed for the foam injection experiments at 70 °C and 8 MPa. Figure 5 showed the photograph of 3-D tank and the inner dimension was 150 mm × 150 mm × 150 mm. There are nine simulation wells in the tank and three electrode pairs are distributed on every simulation well. Resistance values of 27 electrode pairs can be measured through resistivity measuring device. As resistance values were obtained, the saturation of SC-CO_2 in the tank was calculated through the following Archie's equation:

$$I = \frac{R_t}{R_o} = \frac{b}{S_w^n},$$

where R_o is the resistivity at full saturation, R_t is the resistivity at saturation S_w, n is the saturation exponent and b is the coefficient.

Imaging software is used to describe the distribution of gas and surfactant solution inside the tank. Figure 6 presented the schematic of experimental apparatus used for

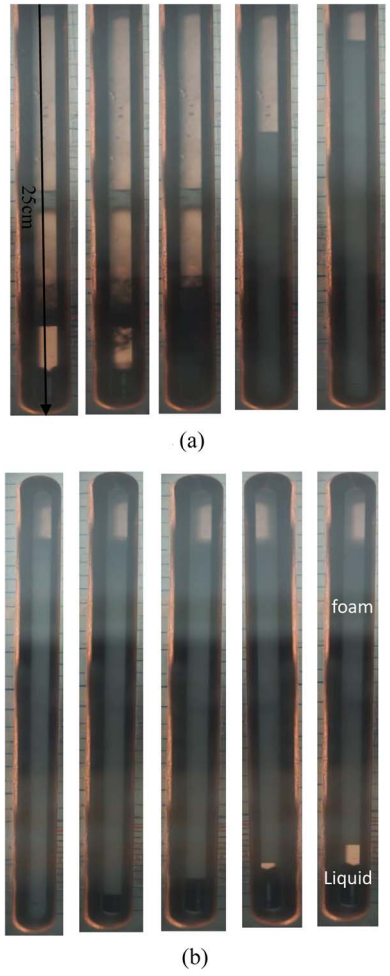

Fig. 2. The foaming and drainage processes at high temperature and pressure conditions. (a) The foaming process; (b) The drainage process.

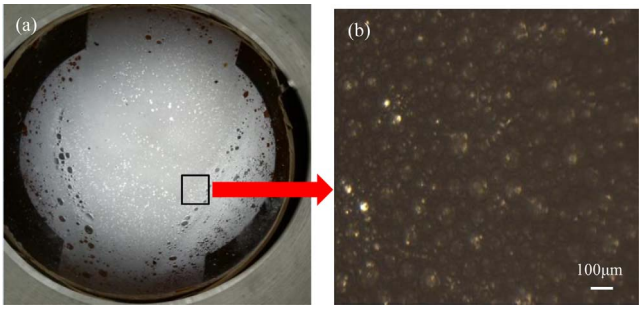

Fig. 3. SC-CO_2 foam in the optical cell (a), the micrographs of SC-CO_2 foam (b).

3-D foam experiments. A heterogeneous 3-D sand pack was prepared by using sand of 100 screen meshes. High permeability layer was packed in the middle part of the tank by using sand of 40 screen meshes. Because permeability and pore volume of 3-D tank is difficult to measure, according to the similarity criterion we used the same size sand to prepare 1-D sand packs to simulate the 3D-tanks. And it was used for measuring the permeability and pore volume. The total flow rate, temperature and back pressure was set at 5 mL/min, 70 °C and 8 MPa.

3 Results and discussion

3.1 Foaming properties of SC-CO_2 foam at different conditions

3.1.1 Effect of surfactant concentration

When the foaming agents were injected into the reservoir, the surfactant solutions would suffer from adsorption and dilution, leading to reduction of effective concentration of foam agents (Chen and Zhao, 2015). Therefore, the effect of surfactant concentration on the foaming properties was evaluated at elevated temperature and pressure. Figure 7a showed the evolution of drainage volume with time (dotted lines represented experimental values and solid line represented fitted curve). It was found that there was an apparent positive linear correlation between drainage volume and drainage time. Drainage rate was equal to the ratio of drainage volume to drainage time. Therefore, we could obtain the drainage rate based on the slope of the curved liner. Figure 7b showed the results of drainage rate with surfactant concentration. Figure 8 summarized the effect of surfactant concentration on foaming volume. It can be seen that the surfactant concentration has little effect on foaming volume, which ranged from 500 mL to 600 mL as surfactant concentration was increased from 0.03% to 1%. However, drainage rate was considerably affected by the surfactant concentration. When surfactant concentration ranged from 0.03% to 0.1%, the drainage rate declined sharply from 22.3 mL/min to 6.4 mL/min. After the surfactant concentration was more than 0.1%, the drainage rate decreased slowly and the value changed from 6.4 mL/min to 3.3 mL/min. As the surfactant solutions flowed through the porous media, rock adsorption and dilution of formation water can reduce the effective surfactant concentration. Therefore, surfactant concentration must be more than 0.1%. Otherwise, the drainage rate would increase greatly due to the decrease of surfactant concentration. When the surfactant concentration was more than 0.3%, the foaming volume and drainage rate changed slightly. Therefore, considering the cost, the surfactant concentration was set at 0.3%.

The decrease of drainage rate with increasing surfactant concentration could be explained by the Critical Micelle Concentration (CMC) (Andrianov *et al.*, 2012). The interfacial tension *versus* log HHSB concentration was displayed in Figure 9. The CMC at which the two lines intersect was about 0.05% (WT) and above CMC the interfacial tension kept nearly constant. Above the CMC, the surfactant adsorption at the water–CO_2 interface reached a saturated state and other excess surfactant molecules may aggregate and form large numbers of spherical micelles in bulk solution. Due to the monolayer adsorption of surfactant molecules, gas–liquid interface became viscoelastic. Interfacial viscosity was different from the bulk viscosity. Interface

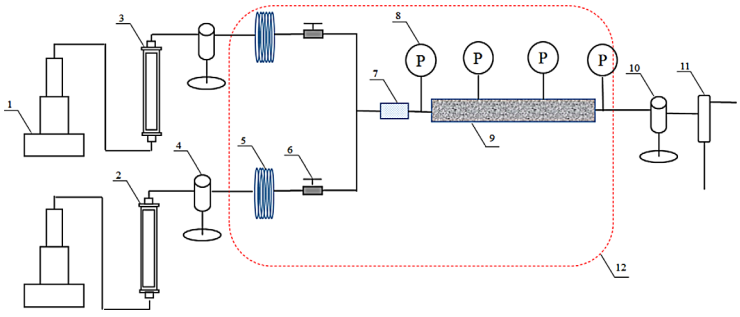

Fig. 4. The apparatus for core flooding experiments. (1) ISCO pump; (2) Gas intermediate container; (3) Liquid intermediate container; (4) Back pressure regulator; (5) Heat exchangers; (6) Valve; (7) Foam generator; (8) Pressure transducer; (9) Natural core; (10) Back pressure regulator; (11) Gas–liquid separator; (12) Oven.

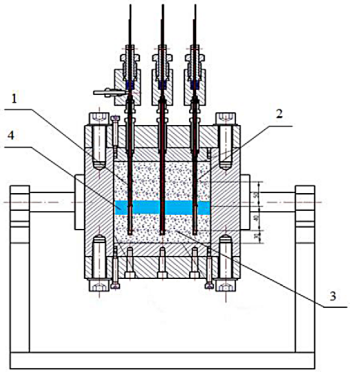

Fig. 5. The schematic diagram of 3-D sand packing model. (1) Simulation well; (2) Electrode pairs; (3) Sand; (4) High permeability layer.

Fig. 6. Photograph of the 3-D sand packing model.

viscosity was referred to the viscosity at gas and liquid interface, which can decrease the moving rate of surfactant molecules (Langevin, 2000). Bulk viscosity meant the viscosity of aqueous solution, which could reduce the drainage rate of foam film. The effect of surfactant concentration on bulk viscosity was shown in Figure 10. It is known that when the surfactant concentration is greater than the Critical Micelle Concentration (CMC), more spherical micelles were formed in aqueous solutions, thereby leading to a higher solution viscosity. Therefore, the bulk viscosity was increased with the increase of surfactant concentration. The higher bulk viscosity resulted in a greater foam stability.

The microstructure of SC-CO_2 foam and average bubble size as a function of time were presented in Figure 11 at 70 °C and 8 MPa when surfactant concentration was 0.3%. It can be seen that the size of SC-CO_2 foam grew gradually and the average bubble size was increased from 68.17 to 84.26 μm as aging time increased from 1 to 6 min. Foam coarsening was attributed to the gas diffusion through the foam lamellae from small bubbles into neighboring larger bubbles (Heller and Kuntamukkula, 1987). The gas diffusion between small bubbles and large bubbles across the film led to foam coarsening and lower bubble density, which was known as Ostwald ripening (Huh and Rossen, 2008).

3.1.2 Effect of temperature

When SC-CO_2 foam was applied for the control of gas mobility at high temperature reservoirs, the foam stability would be challenged. Effect of temperature on film drainage rate and foaming volume was investigated at a fixed pressure of 8 MPa. Figure 12a showed the evolution of drainage volume with time, and according to the fitted equations, Figure 12b showed the drainage rate as a function of temperature. Figure 13 displayed the effect of temperature on foaming volume of SC-CO_2 foam. It can be seen that foaming volume decreased slightly with an increase of temperature whereas drainage rate was reduced greatly as temperature was improved from 40 °C to 120 °C. In particular, when the temperature was increased to 120 °C, the drainage rate was increased dramatically to 8.58 mL/min from 5.22 mL/min at 100 °C. Therefore, it is suggested that the SC-CO_2 foam was applied for the reservoirs with temperature below 100 °C.

High temperature can weaken the interactions among surfactant molecules and affect surfactant adsorption on the lamella. Part of surfactant molecules adsorbed at the CO_2/Water interface will move towards aqueous phase, thereby leading to surfactant density fluctuation and formation of holes on the lamella, which was formed in the gas–liquid lamella due to spatial fluctuations (interfacial waves or dimples) and surfactant density fluctuations (Adkins *et al.*, 2010). The increased desorption of surfactant at the CO_2/Water interface was supported by the increase in interfacial tension of the binary water–CO_2 system with

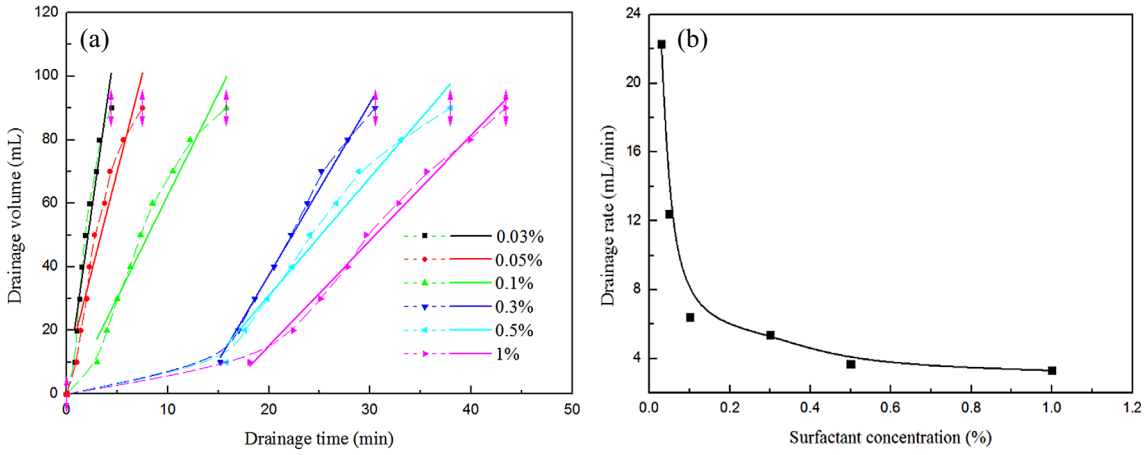

Fig. 7. Evolution of drainage volume with time (a) and drainage rate as a function of surfactant concentration (b) at 70 °C and 8 MPa.

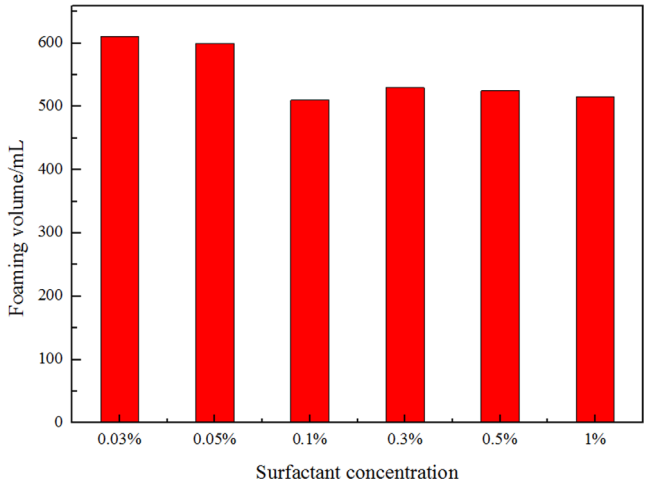

Fig. 8. Effect of surfactant concentration on foaming volume of SC-CO_2 foam at 70 °C and 8 MPa.

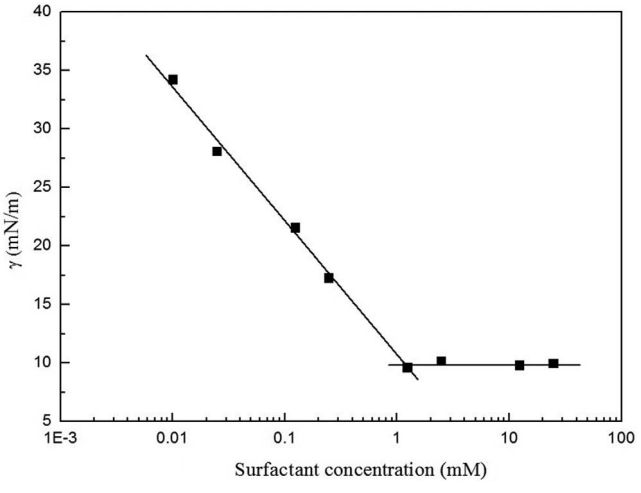

Fig. 9. Interfacial Tension (IFT) between SC-CO_2 and surfactant solution with surfactant concentration at 70 °C and 8 MPa.

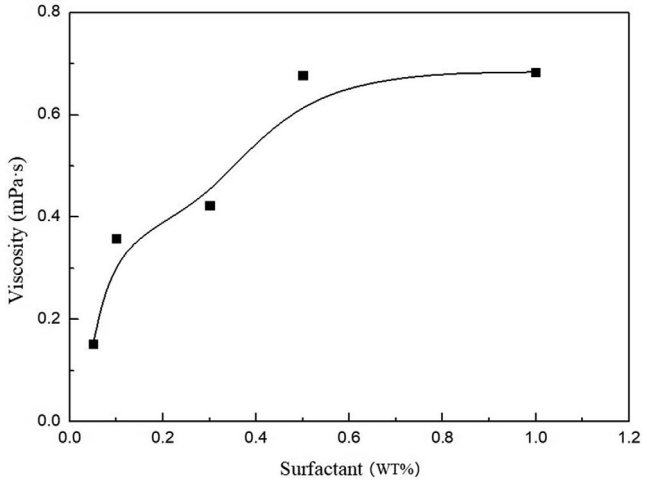

Fig. 10. The effect of surfactant concentration on bulk viscosity of surfactant solution at 70 °C and 8 MPa.

an increase of temperature (as shown in Fig. 14). Higher interfacial tension for the binary water–CO_2 system may promote the surfactant density fluctuation and expand the hole on the lamellae, which will accelerate film drainage and gas transfer between bubbles (Dhanuka *et al.*, 2006). The effect of temperature on the bulk viscosity of the aqueous surfactant solutions was measured at the fixed pressure of 8 MPa and the results were shown in Figure 15. The results showed that the apparent viscosity of surfactant solutions was reduced with the increase of temperature. The decrease of apparent viscosity will accelerate the drainage rate, thereby leading to the rupture of foam film.

3.1.3 Effect of pressure

The effect of pressure on foaming capacity was evaluated at 70 °C with pressure ranging from 4 MPa to 12 MPa. When the pressure was lower than 7.38 MPa, it is gaseous CO_2 foam rather than SC-CO_2 foam. Figure 16a showed the

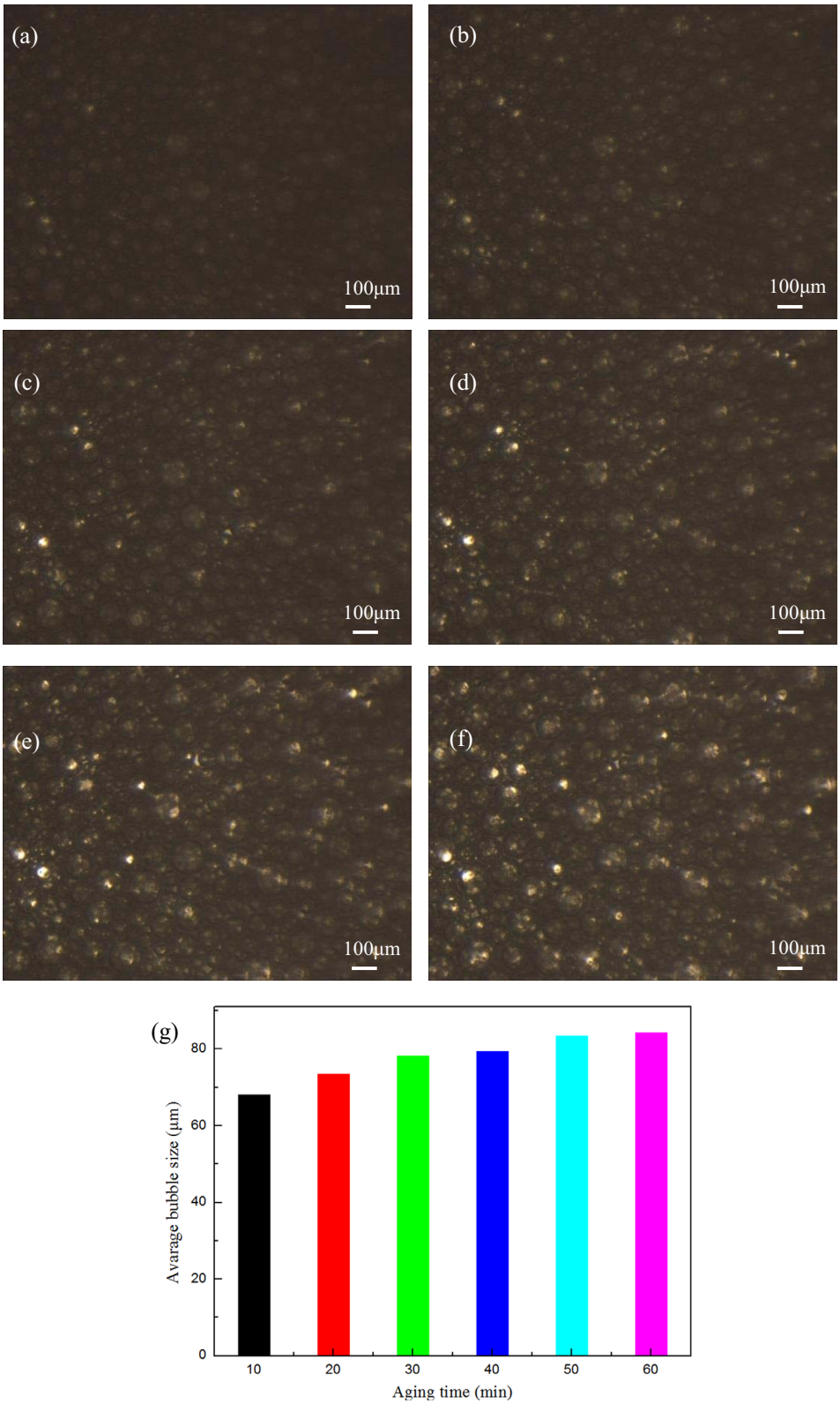

Fig. 11. Microstructure of SC-CO_2 foam at 70 °C and 8 MPa as a function of time at (a) 1 min, (b) 2 min, (c) 3 min, (d) 4 min, (e) 5 min, (f) 6 min and (g) average bubble size.

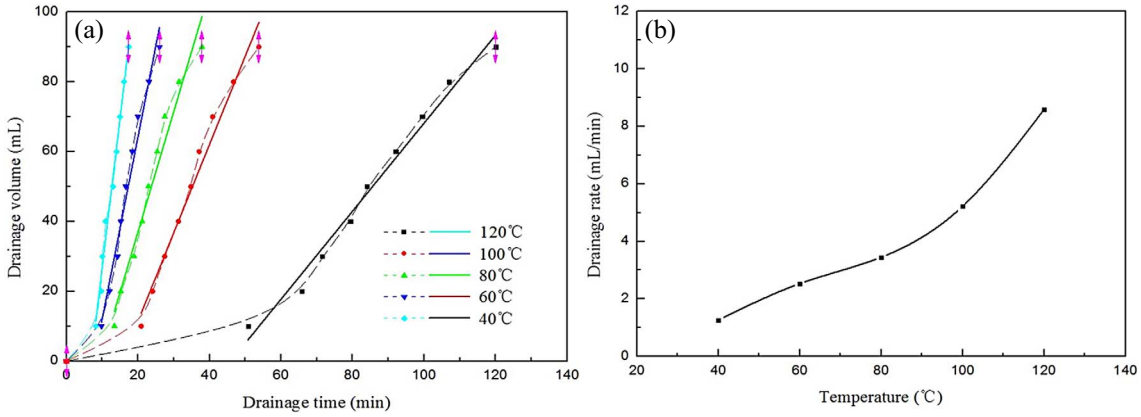

Fig. 12. Evolution of drainage volume of SC-CO_2 foam with time (a) and drainage rate as a function of temperature (b) at 8 MPa.

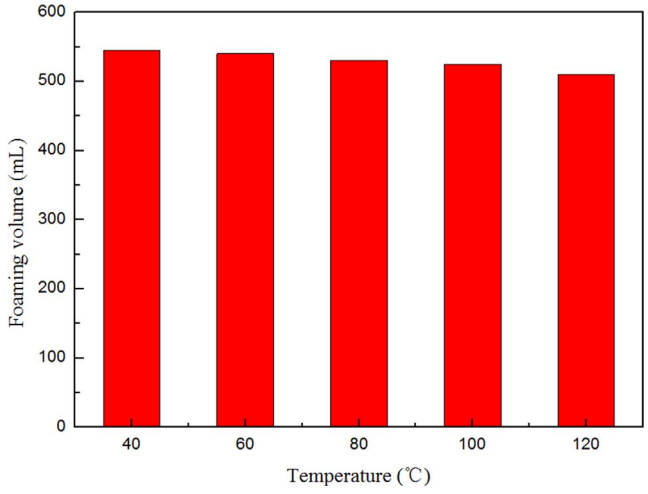

Fig. 13. Effect of temperature on foaming volume of SC-CO_2 foam at 8 MPa.

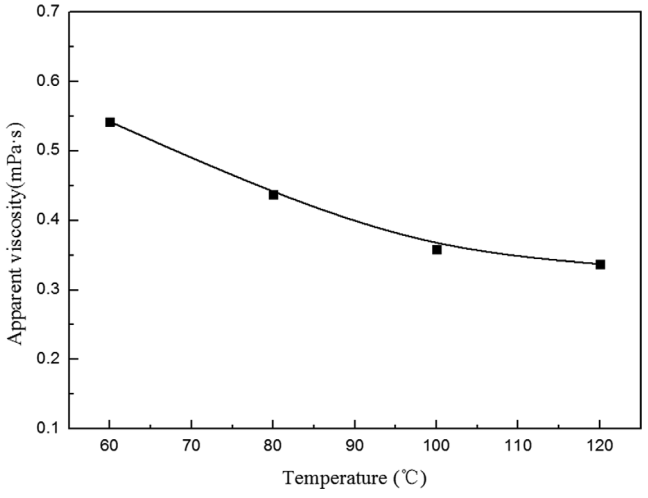

Fig. 15. The effect of temperature on the bulk viscosity of surfactant solutions at 8 MPa when the surfactant concentration was 0.3%.

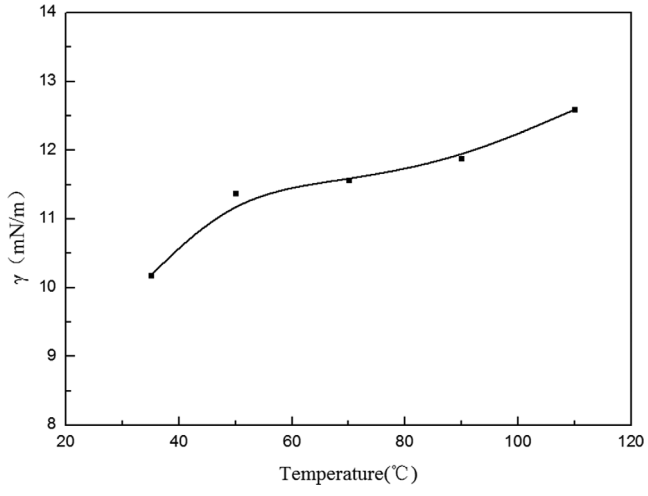

Fig. 14. Interfacial Tension (IFT) between SC-CO_2 and surfactant solution with increase of temperature at 8 MPa when the surfactant concentration was 0.3%.

drainage volume of CO_2 foam with time at different pressures, and based on the fitted equations Figure 16b showed a plot of drainage rate *versus* pressure. Figure 17 illustrated evolution of foaming volume with pressure. It can be seen that foaming volume increased from 490 mL to 590 mL and the drainage rate decreased from 6.76 mL/min to 1.48 mL/min. Therefore, it can be concluded that an increase of pressure can improve both foaming volume and foam stability.

Due to the constant volume of high pressure view cell, CO_2 density increased with increasing pressure. The much higher density meant more CO_2 molecules were involved in formation of CO_2 foam, which led to the increase of foaming volume. An increase in CO_2 density with pressure will also contribute to a considerable increase of the foam stability (Zhang *et al.*, 2013). The much lower density difference between CO_2 and aqueous solution would reduce the drainage rate due to the gravity. In order to further explain the effect of pressure on foam stability, interfacial tension between CO_2 and surfactant solutions were measured as a function of pressure. Figure 18 showed that the

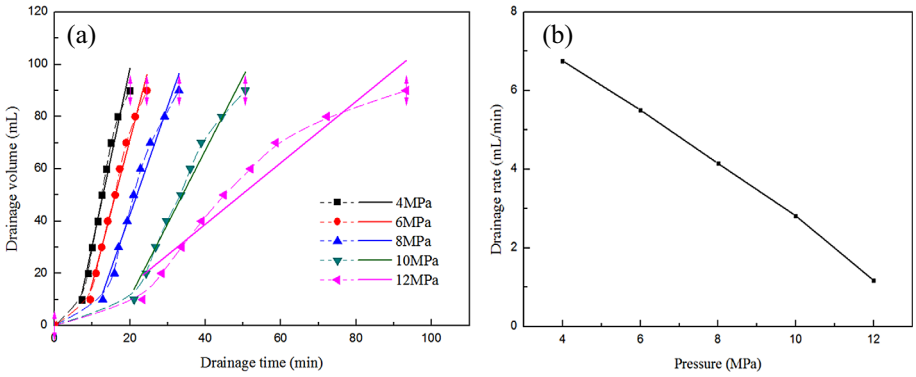

Fig. 16. Evolution of drainage volume of CO_2 foam with time (a) and drainage rate as a function of pressure (b) at 70 °C.

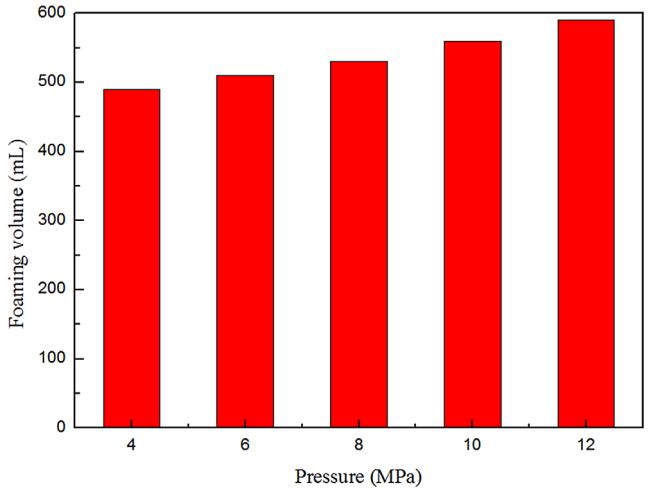

Fig. 17. Effect of pressure on foaming volume of SC-CO_2 foam at 70 °C.

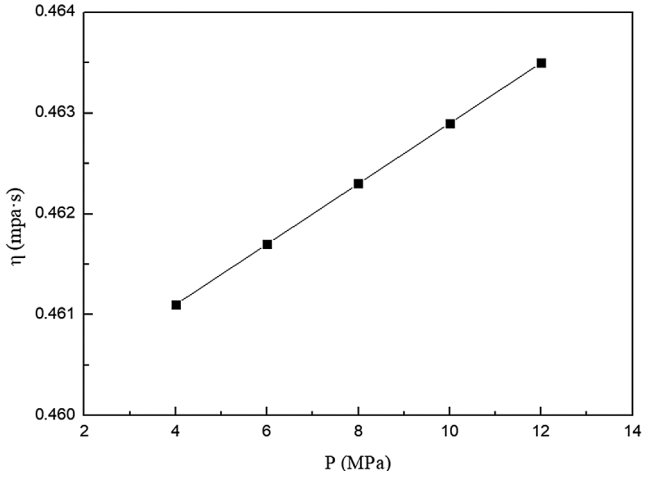

Fig. 19. The effect of pressure on bulk viscosity of surfactant solution at 70 °C.

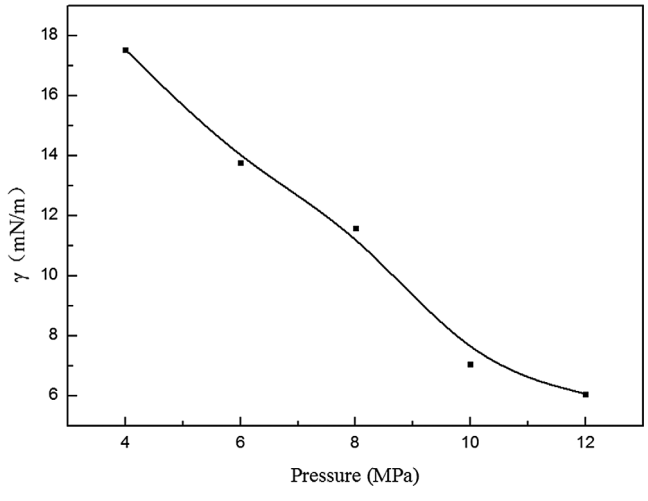

Fig. 18. Interfacial Tension (IFT) between CO_2 and surfactant solution with increase of pressure at 70 °C when the surfactant concentration was 0.3%.

decrease in interfacial tension between CO_2 and aqueous solution with increase of pressure. As the density of CO_2 is increased with increasing pressure, CO_2 has better solvent strength for surfactant tails and surfactant molecules are transferred from aqueous solutions onto gas–liquid interface, which leads to an increase in adsorption of surfactant molecules at the gas–liquid interface and an decrease in interfacial tension (Adkins *et al.*, 2007; Rocha *et al.*, 1999). Lower surface tension and greater surfactant adsorption lead to greater repulsive steric interactions (Rocha *et al.*, 1999). The larger steric repulsion causes the increase of disjoining pressure between foam films which include repulsive interactions (electrostatic, steric and structural interactions) and van der Waals attraction, thereby leading to stable foam lamellae (Exerowa *et al.*, 1987). Figure 19 showed the effect of pressure on the aqueous phase of bulk foam. It can be seen that pressure affected the solution viscosity slightly and the viscosity increased slightly with the increase of pressure. Therefore, the enhancement of foam stability with increase of pressure was mainly attributed to the gas–liquid interface, which was packed with more surfactant molecules due to the high pressure. A larger

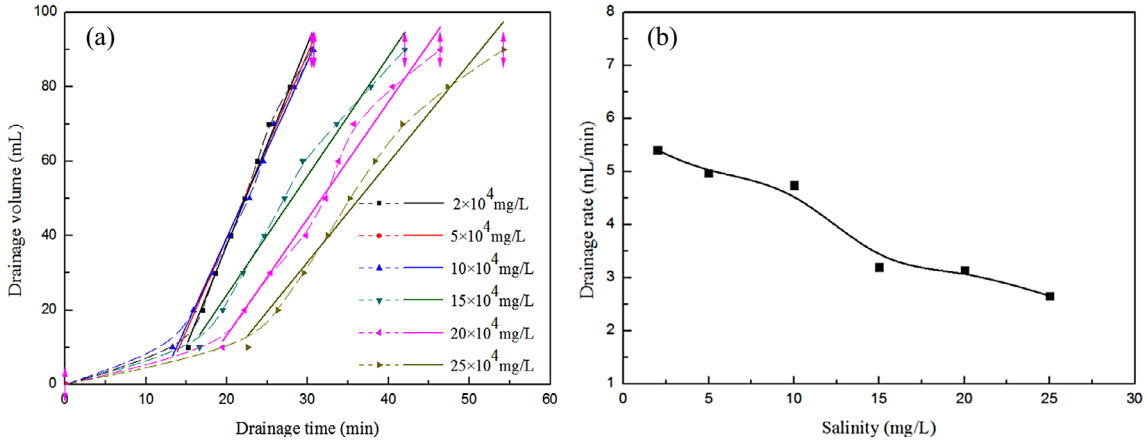

Fig. 20. Evolution of drainage volume of SC-CO_2 foam with time (a) and drainage rate as a function of salinity (b) at 70 °C and 8 MPa.

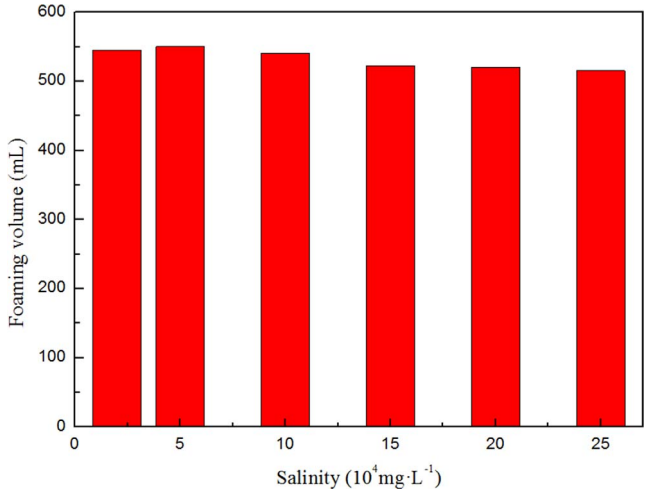

Fig. 21. Effect of salinity on foaming volume of SC-CO_2 foam at 70 °C and 8 MPa.

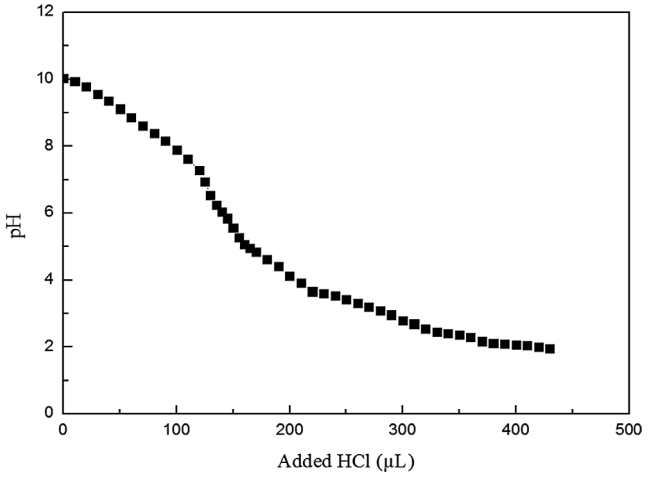

Fig. 22. Change of pH value of surfactant solutions with addition of HCl.

adsorption of surfactant and a lower interfacial tension led to the higher foam stability.

3.1.4 Effect of salinity

The formation water in reservoirs usually contains specific level of salt and divalent ions, and especially divalent ions such as Ca^{2+} and Mg^{2+} have a great influence on foam stability. Figure 20a showed the effect of salinity on foaming volume of SC-CO_2 foam, and based on the fitted equations drainage rate *versus* salinity were shown in Figure 20b. Figure 21 displayed the foaming volume as a function salinity. And it can be seen that the foaming volume decreased slightly whereas the drainage rate declined as salinity was increased from 2×10^4 to 25×10^4 mg/L. It is known that the addition of NaCl and $CaCl_2$ would decrease the foam stability due to the screening of electrostatic repulsion between foam lamellaes. However, from the experimental results of drainage rate with salinity, it can be inferred that the increase of salinity will enhance the foam stability. This may be attributed to the cationic form of betaine surfactants in the aqueous solutions saturated with CO_2.

When the pressure was increased to 8 MPa, the pH of binary water-CO_2 system would decrease to about 4 (Meyssami *et al.*, 1999). From Figure 22 it can be concluded that the isoelectric point of the betaine surfactant was about 6 and thus the betaine surfactant was positive charged. Therefore, due to the large electrostatic repulsion between surfactants, the arrangement of surfactant molecules at the gas–liquid interface was not compact. However, when large amount of salt was added into the aqueous solutions, the headgroup repulsions of betaine surfactant can be screened by the counterions Cl^{-1}. This would increase packing density of surfactant molecules at the gas–liquid interface, thereby producing a stable foam lamellae (Worthen *et al.*, 2014). This hypothesis was verified by decrease of the interfacial tension between SC-CO_2 and aqueous solution with an increase of salinity as shown in Figure 23. Figure 24 shows the viscosity of surfactant solutions with different salinities at 70 °C and 8 MPa. Because of the

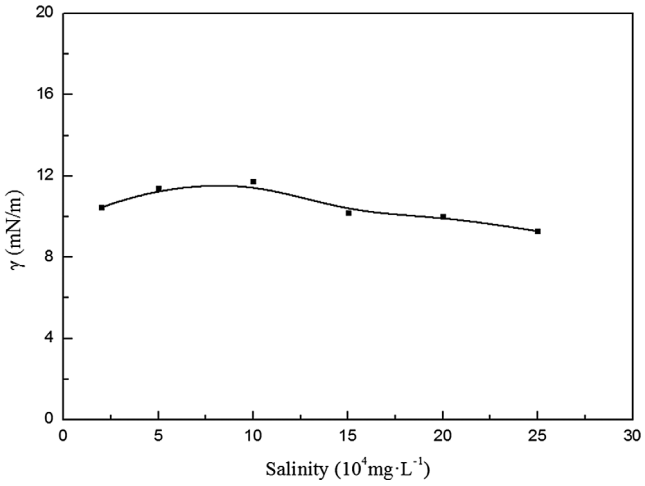

Fig. 23. Interfacial Tension (IFT) between SC-CO_2 and surfactant solution with increase of salinity at 70 °C and 8 MPa when the surfactant concentration was 0.3%.

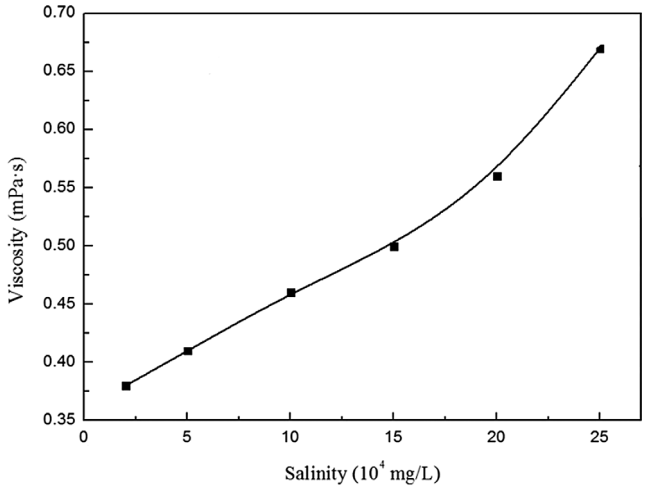

Fig. 24. The effect of salinity on bulk viscosity of surfactant solution at 70 °C and 8 MPa.

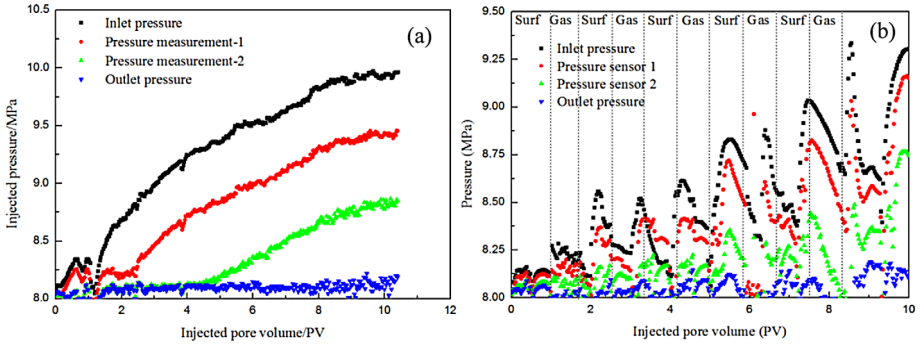

Fig. 25. Multi-point pressure measurements for SCG (a) and SAG (b) methods.

partial miscibility between water and CO_2, the effect of CO_2 solubility in water on the surfactant solution viscosity was neglected (Wiebe, 1941). With the increase in the salinity, the viscosity of the surfactant solutions increased, thereby resulting in the increase of film stability. The increase of viscosity may be attributed to the formation of more micelles because salt ions can screen the electrostatic repulsive interactions between surfactant molecules.

3.2 The flow behaviors of CO_2 foam in 1-D core flooding experiment

The generation and propagation behaviors of SC-CO_2 foam in the porous media were investigated by the multi-point pressure measurement experiment. The experiment was conducted by using two foam injection methods, including SAG and CSG. The core permeability was 300 mD and porosity was about 20%. The length and cross-section area were 30 cm and 4.9 cm^2, separately. Figure 25 showed the evolution of pressure as a function of injected pore volume as measured by different pressure taps at 70 °C and 8 MPa. It can be seen that flow behaviors of SC-CO_2 foams in the porous media were different greatly in terms of the injection method. For the two injection methods, the pressure of the two pressure taps along the core increased sequentially with the foam flow in the porous media.

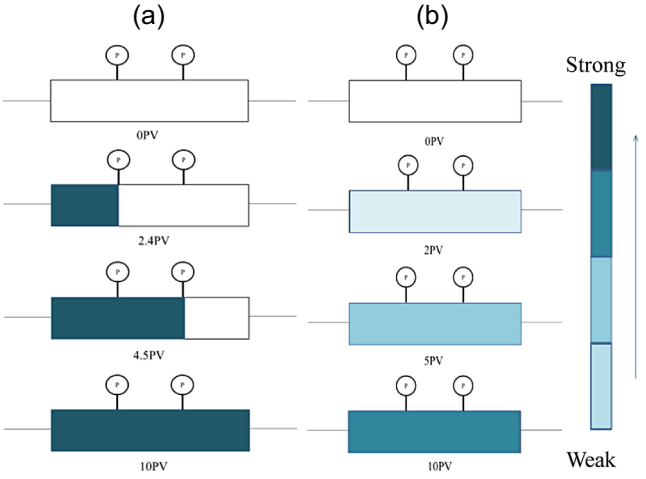

Fig. 26. Propagation mechanism of SC-CO_2 foam in the porous media for CSG method (a) and SAG method (b).

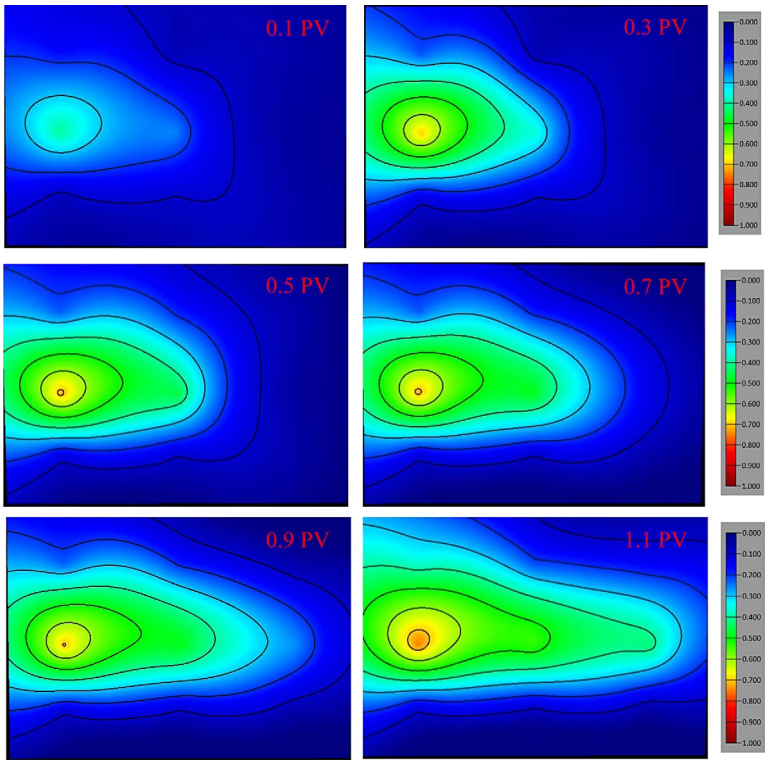

Fig. 27. SC-CO_2 distribution along the diagonal cross section of 3-D tank in the WAG process at 70 °C and 8 MPa.

Comparing the pressures of the two methods, the foam generated by CSG method led to higher pressure at different pressure taps than that of the SAG method, which indicated that co-injection method would generate the stronger foam than SAG method. Besides, it can be seen that propagation rate of the SC-CO_2 foam by SAG method was faster than that of the CSG method. In the SAG case, the pressure of both pressure tap 1 and pressure tap 2 rose at 2 PV, separately. But in the CSG case, it can be noted that the pressure of pressure tap 1 and tap 2 increased at 2.4 PV and 4.5 PV, separately. It indicated that SAG process showed better in-depth propagation and can reduce the gas mobility in deep zone of low permeability reservoirs.

Based on the above results, the propagation mechanisms of SC-CO_2 foam in the porous media were shown in Figure 26 for CSG method and SAG method. The strength of SC-CO_2 foam generated by CSG method was considerably high, forming foam bank in the porous media. With the coinjection of CO_2 and surfactant solution, the foam bank propagated at a piston-like manner in the porous media until the porous media was filled with SC-CO_2 foam (Fig. 26a; Raza, 1970). For SAG method, SC-CO_2 was easy to migrate to the end of the core with the gas flow. Low strength of foam was generated in the most whole core when SC-CO_2 was in contact with surfactant solution. The foam distribution increased spontaneously along the core (Fig. 26b) and accordingly the pressure along the core increased. For the foam implementation in the field, CO_2 foam formed by CSG is easily trapped in the near wellbore area due to the strong foam strength and poor migration ability. Foam formed by CSG method is relatively better for the low permeability reservoir. Surfactant can selectively enter the high permeability layer and meet with subsequent injected CO_2 to form foam. Due to the better propagation capacity, the foam formed by CSG method can migrate to the deep part of the reservoir.

3.3 The mobility control of supercritical CO_2 foam in homogeneous 3-D sand packing tank

Figures 27 and 28 showed the SC-CO_2 distribution along the diagonal cross section as a function of injected pore volume for Water-Alternative-Gas (WAG) and SAG process. During WAG process (Fig. 27), the injected SC-CO_2 flowed through high permeability layers due to model heterogeneity and early CO_2 break through occurred at about 0.9 PV. After 1.1 PV SC-CO_2 was injected, a high proportion of the tank was still not swept by SC-CO_2. In the CO_2 flooding reservoirs, CO_2 channeling resulted in large amount of oils remained in the unswept areas and resulted in low oil-recovery efficiency. During SAG process (Fig. 28), SC-CO_2 foam was formed as the SC-CO_2 displaced the surfactant solution, which could reduce the CO_2 mobility and increase the volumetric sweep efficiency of SC-CO_2. After 1.1 PV SC-CO_2 was injected, most part of the tank was swept by SC-CO_2. Figure 25 showed the SC-CO_2 saturation along the diagonal cross section as a function of injected pore volume. It can be seen that SC-CO_2 saturation in the SAG process was larger than that in the WAG process while SC-CO_2 was injected into the tank.

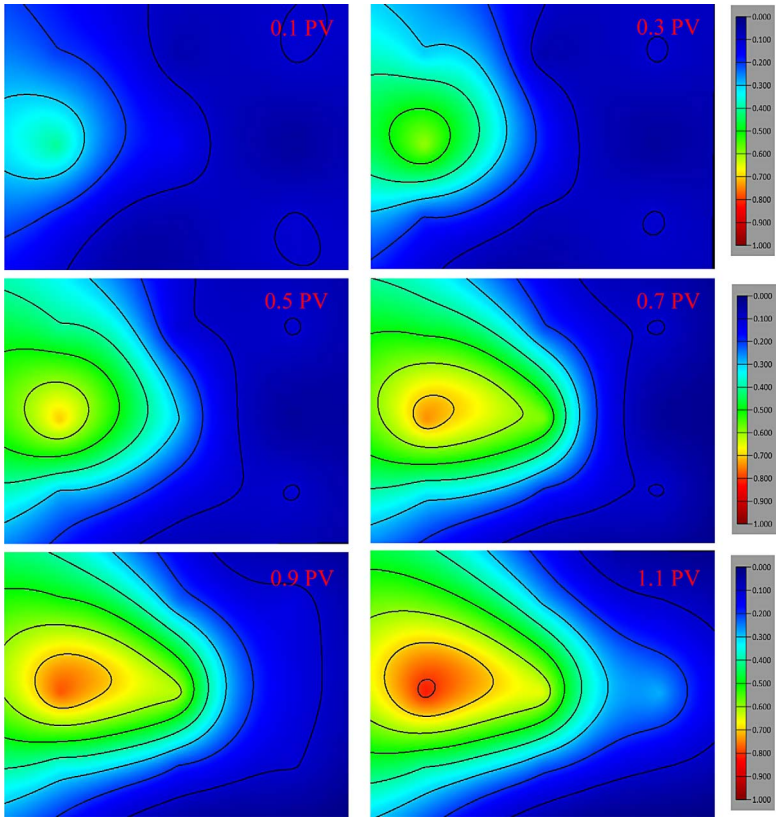

Fig. 28. SC-CO_2 distribution along the diagonal cross section of 3-D tank in the SAG process at 70 °C and 8 MPa.

4 Conclusion

In this work, a temperature resistant and salt resistant surfactant, HHSB was screened to stabilize SC-CO_2 foam during CO_2 flooding. Effects of surfactant concentration, pressure and salinity on film drainage rate and foam stability were investigated under high temperature and pressure conditions. With the increase of surfactant concentration (above CMC), the spherical micelles were formed in the solutions to enhance the surface viscosity, thereby increase film stability. An increase of pressure would increase solvent strength of SC-CO_2 for surfactant tails and decrease the interfacial tension to enhance foam stability. In aqueous solutions saturated with SC-CO_2 at high pressure, the betaine surfactant was transformed into the cationic protonated form. An increase of salinity could decrease electrostatic repulsion between surfactants and lead to denser surfactant pack at C/W interface. Core flooding experiments showed that compared to that of CSG, SC-CO_2 foam formed by SAG has a better in-depth migration capacity but had lower foam strength. The heterogeneous sand pack model was developed to verify that SC-CO_2 foam could reduce the CO_2 mobility and improve the sweep efficiency of CO_2 under high temperature and salinity conditions.

Acknowledgments. This work was supported by the National Science and Technology Major Project (Grant No. 2016ZX05016004), the Key State Science and Technology Project (Grant No. 2017ZX05030) and the PetroChina Science and Technology Major Project (Grant No. 2016B-1304).

References

Adkins S.S., Chen X., Chan I., Torino E., Nguyen Q.P., Sanders A.W., Johnston K.P. (2010) Morphology and stability of CO_2-in-water foams with nonionic hydrocarbon surfactants. *Langmuir ACS J. Surf. Coll.* **26**, 8, 5335–5348.

Adkins S.S., Gohil D., Dickson J.L., Webber S.E., Johnston K.P. (2007) Water-in-carbon dioxide emulsions stabilized with hydrophobic silica particles. *Phys. Chem. Chem. Phys.* **9**, 48, 6333–6343.

Al Ayesh A.H., Salazar R., Farajzadeh R., Vincent-Bonnieu S., Rossen W.R. (2017) Foam diversion in heterogeneous reservoirs: effect of permeability and injection method. *SPE J.* **22**, 05, 1402–1415.

Andrianov A., Farajzadeh R., Mahmoodi Nick M., Talanana M., Zitha P.L. (2012) Immiscible foam for enhancing oil recovery: bulk and porous media experiments. *J. Ind. Eng. Chem.* **51**, 5, 2214–2226.

Basheva E.S., Ganchev D., Denkov N.D., Kasuga K., Satoh N. Tsujii K. (2000) Role of betaine as foam booster in the presence of silicone oil drops. *Langmuir* **16**, 3, 1000–1013.

Chen Z., Zhao X. (2015) Enhancing heavy-oil recovery by using middle carbon alcohol-enhanced waterflooding, surfactant flooding, and foam flooding, *Energy Fuels* **29**, 4, 2153–2161.

Da C., Alzobaidi S., Jian G., Zhang L., Biswal S.L., Hirasaki G.J., Johnston K.P. (2018) Carbon dioxide/water foams stabilized with a zwitterionic surfactant at temperatures up to 150 °C in high salinity brine. *J. Ind. Eng. Chem.* **166**, 880–890.

Danov K.D., Kralchevska S.D., Kralchevsky P.A., Ananthapadmanabhan K.P., Lips A. (2004) Mixed solutions of anionic and zwitterionic surfactant (betaine): Surface-tension isotherms, adsorption, and relaxation kinetics. *Langmuir* **20**, 13, 5445–5453.

Dhanuka V.V., Dickson J.L., Ryoo W., Johnston K.P. (2006) High internal phase CO_2-in-water emulsions stabilized with a branched nonionic hydrocarbon surfactant, *J. Colloid. Interf. Sci.* **298**, 1, 406–418.

Du D., Li Y., Chao K., Wang C., Wang D. (2018) Laboratory study of the Non-Newtonian behavior of supercritical CO_2 foam flow in a straight tube. *J. Ind. Eng. Chem.* **164**, 390–399.

Emera M.K., Sarma H.K. (2005) Use of genetic algorithm to estimate CO_2 – oil minimum miscibility pressure – a key parameter in design of CO_2 miscible flood, *J. Petrol. Sci. Eng.* **46**, 1–2, 37–52.

Exerowa D., Kolarov T., Khristov K. (1987) Direct measurement of disjoining pressure in black foam films. I. Films from an ionic surfactant. *Colloids Surf. A Physicochem. Eng. Asp.* **22**, 2, 161–169.

Farid Ibrahim A., Nasr-El-Din H. (2018) Stability improvement of CO_2 foam for enhanced oil recovery applications using nanoparticles and viscoelastic surfactants, in: *SPE Trinidad and Tobago Section Energy Resources Conference. Port of Spain, Trinidad and Tobago*, Society of Petroleum Engineers, 17 p.

Friedmann F., Chen W.H., Gauglitz P.A. (1991) Experimental and simulation study of high-temperature foam displacement in porous media. *SPE Reserv. Eng.* **6**, 01, 37–45.

Ge J., Wang Y. (2015) Surfactant enhanced oil recovery in a high temperature and high salinity carbonate reservoir. *J. Surfactants Deterg.* **18**, 6, 1043–1050.

Ghasemi M., Astutik W., Alavian S., Whitson C.H., Sigalas L., Olsen D., Suicmez V.S. (2018) Experimental and numerical investigation of tertiary-CO_2 flooding in a fractured chalk reservoir, *J. Pet. Sci. Eng.* **164**, 485–500.

Golemanov K., Denkov N.D., Tcholakova S., Vethamuthu M., Lips A. (2008) Surfactant mixtures for control of bubble surface mobility in foam studies. *Langmuir* **24**, 9956–9961.

Heller J.P., Kuntamukkula M.S. (1987) Critical review of the foam rheology literature. *Ind. Eng. Chem. Res.* **26**, 2, 318–325.

Hirasaki G.J., Lawson J.B. (1985) Mechanisms of foam flow in porous media: Apparent viscosity in smooth capillaries. *SPE J.* **25**, 02, 176–190.

Holt T., Vassenden F., Svorstol I. (1996) Effects of pressure on foam stability; implications for foam screening, in: *SPE/DOE Improved Oil Recovery Symposium*, Tulsa, Oklahoma, April 1996. https://doi.org/10.2118/35398-MS.

Huh C., Rossen W.R. (2008) Approximate pore-level modeling for apparent viscosity of polymer-enhanced foam in porous media. *SPE J.* **13**, 01, 17–25.

Langevin D. (2000) Influence of interfacial rheology on foam and emulsion properties. *Adv. Colloid. Interface. Sci.* **88**, 1–2, 209–222.

Li B., Hirasaki G.J., Miller C.A. (2006) Upscaling of foam mobility control to three dimensions, in: *SPE/DOE Symposium on Improved Oil Recovery, Tulsa, Oklahoma, USA*, Society of Petroleum Engineers.

Li R.F., Hirasaki G.J., Miller C.A., Masalmeh S.K. (2012) Wettability alteration and foam mobility control in a layered, 2D heterogeneous sandpack, *SPE J.* **17**, 04, 1207–1220.

Li W., Wei F., Xiong C., Ouyang J., Dai M., Shao L., Lv J. (2019) Effect of salinities on supercritical CO_2 foam stabilized by a betaine surfactant for improving oil recovery. *Energy Fuels* **33**, 9, 8312–8322.

Meyssami B., Balaban M.O., Teixeira A.A. (1999) Prediction of pH in model systems pressurized with carbon dioxide. *Biotechnol. Prog.* **8**, 2, 149–154.

Patil P.D., Knight T., Katiyar A., Vanderwal P., Scherlin J., Rozowski P., Ibrahim M., Sridhar G.B., Nguyen Q.P. (2018) *CO_2 Foam Field Pilot Test in Sandstone Reservoir: Complete Analysis of Foam Pilot Response*, SPE Improved Oil Recovery Conference, Tulsa, Oklahoma, USA.

Raza S.H. (1970) Foam in porous media: characteristics and potential applications. *SPE J.* **10**, 04, 328–336.

Ren G., Nguyen Q.P., Lau H.C. (2018) Laboratory investigation of oil recovery by CO_2 foam in a fractured carbonate reservoir using CO_2-soluble surfactants. *J. Ind. Eng. Chem.* **169**, 277–296.

Rocha S.R.P.D., Harrison K.L., Johnston K.P. (1999) Effect of surfactants on the interfacial tension and emulsion formation between water and carbon dioxide. *Langmuir* **15**, 2, 419–428.

Rossen W.R., Van Duijn C.J., Nguyen Q.P., Shen C., Vikingstad A.K. (2010) Injection strategies to overcome gravity segregation in simultaneous gas and water injection into homogeneous reservoirs. *SPE J.* **15**, 01, 76–90.

Wang L., Yoon R.H. (2009) Effect of pH and NaCl concentration on the stability of surfactant-free foam films. *Langmuir* **25**, 1, 294–297.

Wiebe R.J.C.R. (1941) The binary system carbon dioxide-water under pressure, *Chem. Rev.* **29**, 3, 475–481.

Worthen A.J., Parikh P.S., Chen Y., Bryant S.L., Huh C., Johnston K.P. (2014) Carbon dioxide-in-water foams stabilized with a mixture of nanoparticles and surfactant for CO_2 storage and utilization applications. *Energy Procedia* **63**, 7929–7938.

Xue Z., Worthen A., Qajar A., Robert I., Bryant S.L., Huh C., Prodanović M., Johnston K.P. (2016) Viscosity and stability of ultra-high internal phase CO_2-in-Water foams stabilized with surfactants and nanoparticles with or without polyelectrolytes. *J. Colloid Interface Sci.* **461**, 383–395.

Zhang H., Xu G., Liu T., Xu L., Zhou Y. (2013) Foam and interfacial properties of Tween 20 – bovine serum albumin systems, *Coll. Surf. A* **416**, 23–31.